

Nuclear Magnetic Resonance Studies of New Six-Coordinate High-Spin Ferric Porphyrin Complexes as Models for Aquometmyoglobin. 1. Formation of Alcohol-Coordinated Octaethylporphyrin Complexes in Solution

Isao Morishima,* Susumu Kitagawa,¹ Eizo Matsuki, and Toshiro Inubushi²

Contribution from the Department of Hydrocarbon Chemistry, Faculty of Engineering, Kyoto University, Kyoto 606, Japan. Received May 25, 1979

Abstract: A new type of six-coordinate, high-spin ferric porphyrin complex, having as different axial ligands alcohol and amine, has been shown to be formed in CHCl_3 or CH_2Cl_2 solution from octaethylporphyrin chloride. Structural and magnetic characterizations are made by ^1H NMR hyperfine shifts, solution magnetic susceptibility, and optical absorption spectra. In addition to this new complex, $[\text{OEPFe}^{3+}(\text{ROH})(\text{amine})]^+\text{Cl}^-$, we have also studied the complex $[\text{OEPFe}^{3+}(\text{ROH})_2]^+\text{Cl}^-$ in the high-spin ferric state. These new types of six-coordinate high-spin complexes were examined for a variety of alcohols and amines and are also discussed in relation to the models of aquometmyoglobin. The equilibrium constants for the formation of these complexes in solution were also determined.

Introduction

The structural characterization of a wide variety of hemoproteins³⁻⁵ has revealed that the heme moiety is bound to the protein by at least one coordinate bond between the iron and a nitrogen of a histidine residue (imidazole) of the protein. Although the one iron-imidazole linkage appears to be ubiquitous in hemoproteins, there is a great diversity in the ligands located trans to the histidyl imidazole, ranging from none in deoxyhemoglobin (Hb)³ and deoxymyoglobin (Mb),^{3,4} to various ligands such as methionine sulfur^{4,5} in cytochrome *c*, histidyl imidazole^{4,5} in cytochromes *b*₂ and *b*₅, and water^{3,4} in methemoglobin (met-Hb) and metmyoglobin (met-Mb). Hence, structural effects on metal-ligand binding are a central theme in the understanding of the role played by the iron porphyrin center, in various heme proteins, in a variety of biological functions. In an attempt to understand structure-function relationships, many investigations have focused on the correlation between molecular structure in the heme environment, oxidation states, and spin states for model porphyrin complexes.

During the past 10 years, studies on the physicochemical properties⁶⁻¹³ of low-spin ferric porphyrin complexes, with a variety of axial ligands, have provided significant information on the nature of porphyrin-iron and axial ligand-iron binding. Such six-coordinate complexes are also available in naturally occurring systems, such as *b*₂ and *b*₅ type cytochromes,^{4,5} where the existence of two coordinated histidyl imidazoles is well established. On the other hand, high-spin ferric porphyrin complexes have been well known only in the five-coordinated porphyrins,¹⁴⁻¹⁶ such as hemin halides and μ -oxo derivatives, etc. The five-coordinate derivatives have a considerable displacement¹⁷ of the iron atom from the mean plane of the porphyrin ring. This structural feature is potentially useful for studies of the stereochemistry of porphyrin complexes. This proposition has become questionable with the recently reported structure¹⁸ of the bis(aquo-TPP)¹⁹ complex. With this as a start, several other six-coordinate ferric porphyrins²⁰ utilizing weak field ligands, such as sulfoxide, tetramethyl sulfoxide (Me_4SO), and pyridine *N*-oxide, have been synthesized and characterized as ferric high-spin complexes. The X-ray crystal-structure studies revealed that the iron atom is in the heme plane, and the bond distance between the iron and porphyrin core nitrogen atom is unusually large in comparison with normal high-spin ferric porphyrin complexes. Concurrently, NMR studies²¹ in solution have shown that the six-coordinated high-spin ferric porphyrin complex with dimethyl sulfoxide

as the axial ligand, $\text{TPPFe}(\text{Me}_2\text{SO})_2^+$, is formed at low temperature (-70°C). These works imply that six-coordinate high-spin ferric porphyrins can be produced by the use of weak-field ligands.

Six-coordination is frequently encountered in high-spin ferric hemoproteins^{3,5} such as met-Hb and -Mb, etc., which are stable under physiological conditions. Hence, of great interest is the characterization of six-coordinate models for the high-spin met-Hb and -Mb. The major concern in this study is to present the pertinent models for aquomet-Hb and -Mb in which the iron(III) atom is coordinated by water trans to a nitrogenous base of the histidyl imidazole. We are also concerned with the other new type of six-coordinate high-spin ferric porphyrins in solution, which has alcohol in the two axial positions at room temperature. We report herein the structure and dynamic equilibria of the six-coordinate high-spin ferric porphyrins with amine and alcohol as the ligands. These are expected to be appropriate models for aquomet-Hb and met-Mb, since (i) the axial ligands of the heme moiety are structurally analogous in both model and protein systems, and (ii) the present aquomet-Mb model complex is selectively and stably formed with various combinations of amine and alcohol derivatives in solution. A scheme for the complex formation in solution will also be presented.

NMR studies of paramagnetic molecules in solution can afford information on the equilibria associated with ligand binding as well as on the electronic structure of the complex on the basis of isotropic shifts and solution magnetic susceptibilities. Such NMR data for six-coordinate high-spin ferric porphyrins have been lacking except in the case of $\text{TPPFe}(\text{Me}_2\text{SO})_2$.²¹

Here we will examine ligand exchange reactions of porphyrin chloride (PFeCl) in methylene chloride solution in the presence of alcohol and/or aliphatic amine (L). In the case of six-coordinated ferric porphyrin complexes, two steps are possible for the axial ligand addition to an iron atom. The first step is the formation of the 1:1 complex:



with:

$$K_1 = [\text{PFeL}_1\text{Cl}]/[\text{PFeCl}][\text{L}_1] \quad (2)$$

The second step is represented by:



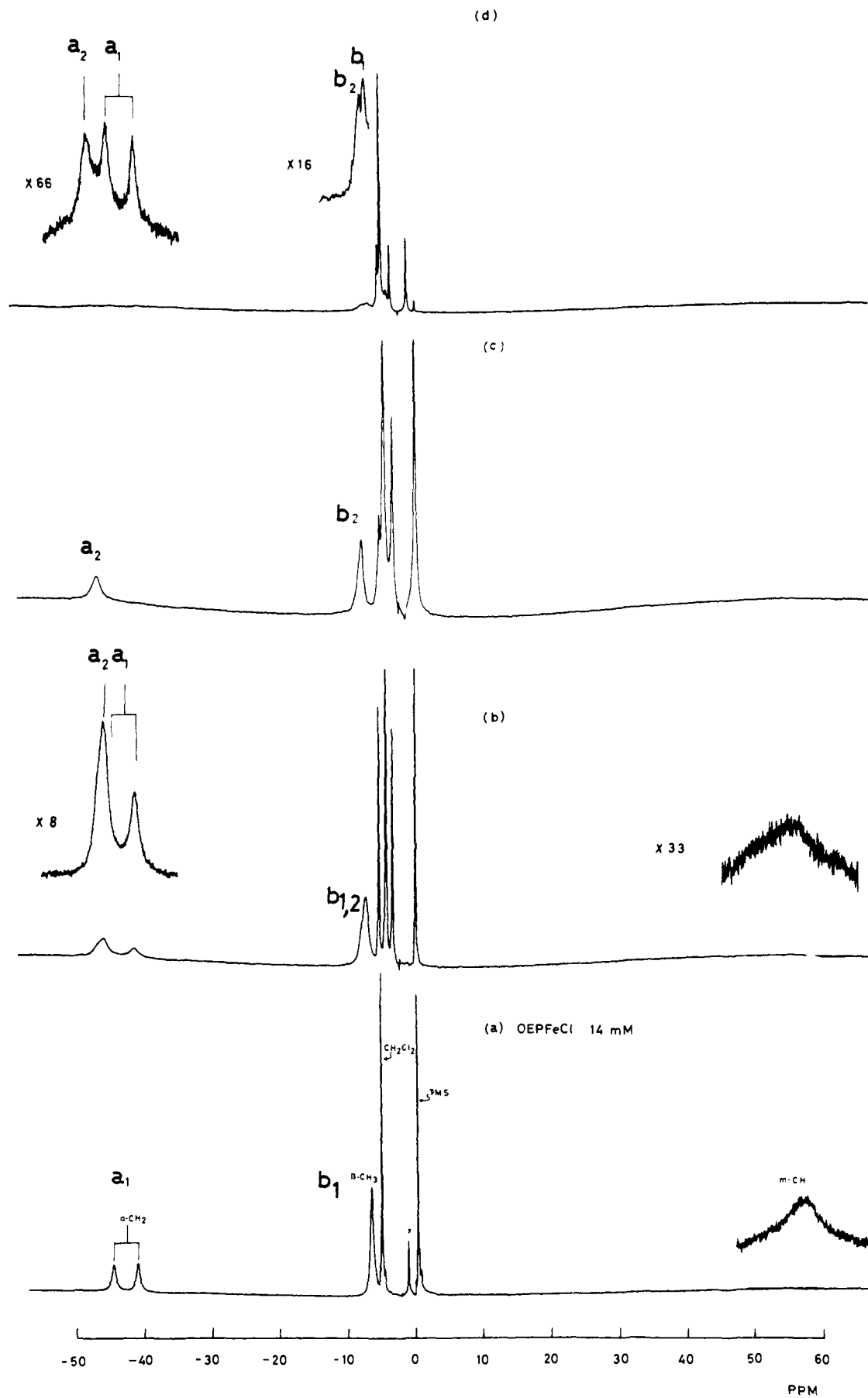


Figure 1. ^1H NMR spectra at 24 °C of: (a) CD_2Cl_2 ; (b) 3:1 $\text{CD}_2\text{Cl}_2/\text{CD}_3\text{OD}$; (c) 3:2 $\text{CD}_2\text{Cl}_2/\text{CD}_3\text{OD}$; and (d) 3:4 $\text{CD}_2\text{Cl}_2/\text{C}_2\text{D}_5\text{OD}$ solutions; $[\text{OEPFeCl}]_0 = 14 \text{ mM}$ for a, b, and c and 5 mM for d. Peaks a_1 and b_1 are the $\alpha\text{-CH}_2$ and $\beta\text{-CH}_3$ resonances for OEPFeCl , respectively. Peaks a_2 and b_2 are the $\alpha\text{-CH}_2$ and $\beta\text{-CH}_3$ resonances for $\text{OEPFe}(\text{ROH})_2^+\text{Cl}^-$, respectively.

with the product, a tight ion pair, and:

$$K_2 = [\text{PFeL}_1\text{L}_2^+\text{Cl}^-]/[\text{PFeL}_1\text{Cl}][\text{L}_2] \quad (4)$$

Low-spin ferric porphyrins with nitrogenous ligands ($L_1 = L_2$) are well documented,^{9,10} and the electronic, steric, and solvation factors that affect the complex stability have been examined. Such low-spin ferric porphyrin complexes with nitrogenous bases have, in general, larger values for K_2 than for K_1 ,¹⁰ and 1:1 complex formation (eq 1) is not always detected. In these cases the reaction follows an apparently single-step process, as given by eq 5:



where

$$\beta_2 = K_1K_2 \quad (6)$$

We are concerned here with the case of $L_1 = \text{amine}$ and $L_2 = \text{alcohol}$, where eq 5 and 6 can be applied to define the coordination stoichiometry.

Experimental Section

Materials. The free porphyrins, H₂OEP and H₂TPP, and their ferric complexes were synthesized according to methods described in the literature.²²⁻²⁴ The final products, OEPFeCl and TPPFeCl, were recrystallized from benzene-chloroform solution. The purity of these complexes was checked optically and by ¹H NMR. The various axial bases, piperidine (pip), pyrrolidine (pyrr), and aziridine (az), were distilled over calcium hydride before use. Methanol-*d*₄ and ethanol-*d*₆, purchased from Merck, were utilized for ¹H NMR spectroscopic studies without further treatment. The alcohols such as methanol, ethanol, and propanol used for optical studies were dried and distilled before use.

¹H NMR Measurements. 220-MHz ¹H NMR spectra were obtained with a Varian HR 220 spectrometer equipped with a Nicolet pulse FT accessory TT-100. Between 512 and 1024 transients were accumulated using a 30-μs (90°) pulse; 2K data points were collected over bandwidths of 30.3 kHz. All of the temperatures were calibrated to an accuracy of ±2 °C using the temperature-dependent difference between the CH₃ and OH shifts of pure methanol. The alcohol and/or amine coordinated complexes were prepared in chloroform-*d* and dichloromethane-*d*₂ solutions. ¹H NMR measurements on very dilute solutions were performed by employing a JEOL FX-100 spectrometer with a homonuclear gated decoupling program.

Solution Magnetic Susceptibilities. These were determined by the method of Evans²⁵ for a sample containing 10 mM complex. The magnetic moment of the paramagnetic adduct was obtained from the separation between the ¹H signals from Me₄Si and the solution of the adduct contained in concentric tubes. This assumes that a single species is formed in solution, which is verified by monitoring the α-CH₂ resonance of OEP and pyrrole-H resonance of TPP.

Equilibrium Constants. Equilibrium constants for the complexes OEPFe(amine)(CH₃OH)⁺Cl⁻ were determined by integration of the α-CH₂ signals of OEPFe(amine)(CH₃OH)⁺Cl⁻, while those for OEPFe(ROH)₂⁺Cl⁻ were determined by optical spectroscopy because of the collapse of two α-CH₂ peaks upon formation of the symmetrical OEPFe(ROH)₂ complex. The detailed analyses are mentioned in the following section.

Electronic Spectral Measurements. Spectrophotometric measurements were made on a Shimadzu 200S spectrometer; 10-mm path length cuvettes were utilized for the measurements. Equilibrium constants were typically measured from the absorbance of ~8 μM OEPFeCl and TPPFeCl solutions.

Results and Discussion

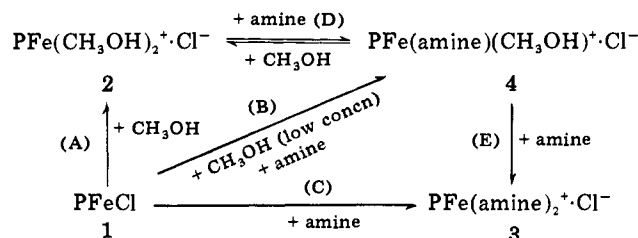
(a) Formation of High-Spin Ferric OEP Complexes Coordinated by Alcohol. In Figure 1 are shown the typical ¹H NMR spectral changes that occur when alcohol (methanol and ethanol) is added to OEPFeCl in CD₂Cl₂ solution. Addition of methanol caused two effects on the spectrum: the porphyrin peripheral β-CH₃ resonance shifted downfield and the meso-H peak shifted upfield, with concomitant line broadening, and

Table I. Observed ¹H NMR Shifts for Some Ferric Octaethylporphyrin Complexes^a

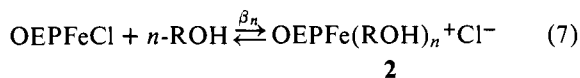
axial ligand	α-CH ₂	β-CH ₃	meso-H
Cl ⁻	-44.5	-40.9	-6.7
CH ₃ OH ^b	-46.9	-7.4	58.7
C ₂ H ₅ OH ^c	-47.6	-7.7	

^a Shifts are in ppm from Me₄Si at 25 °C, in CD₂Cl₂ solution. ^b In CD₂Cl₂-CD₃OD (1:1, v/v) solvent. ^c In CD₂Cl₂-C₂D₅OD (3:4, v/v) solvent.

Scheme I



a new single peak appeared at -47 ppm, as illustrated in Figure 1b. As more methanol was added, the new peak (a₂) increased in intensity at the fixed position. This indicates that chemical exchange between OEPFeCl and the new species is slow enough to afford their proton signals simultaneously. Finally, in the 1:1 CD₂Cl₂/CD₃OD solution the peak a₁ of high-spin OEPFeCl disappeared as shown in Figure 1c. A spectrum similar to Figure 1c was obtained in a very dilute solution of OEPFeCl (~40 μM) in CDCl₃/CD₃OD, indicating that methanol does not influence the aggregation of OEPFeCl. In the case of ethanol (Figure 1d), the peak intensities of the spectrum of OEPFeCl decreased, and another set of resonances appeared and grew in intensity at the fixed position that is displaced from the peak position of pure OEPFeCl, unlike the case of methanol. Thus, the use of different alcohols allows us to assign the new peaks a₂ and b₂ to the α-CH₂ and β-CH₃ proton signals, respectively, of the ferric OEP complex with axially coordinated alcohol molecules. Accordingly, only a single new species (complex 2, Scheme I), designated as OEPFe(ROH)_n⁺Cl⁻, may be formed according to eq 7:



The observed shifts for these proton resonances are given in Table I.

In order to determine the stoichiometry of the formation of complex 2, we have measured the visible spectra. In Figure 2a are shown the typical spectral changes in the 300-460-nm region when methanol is successively added to OEPFeCl in CH₂Cl₂ solution. The resulting two isosbestic points (380 and 400 nm) are also indicative of the equilibrium expressed by eq 7. According to the usual procedure,²⁶ plots of log (A - A₀/A_c - A) vs. log [CH₃OH] were constructed (Figure 2b), where A is the absorbance at the wavelength (390 nm) of interest, A₀ is the absorbance of OEPFeCl in the absence of methanol, and A_c is its absorbance in the presence of a large excess of alcohol. The slope of the linear plot affords the coordination number, n, in eq 7. For methanol, the value of n is 4. The results for all of the complexes studied here are summarized in Table II.

We have also examined the alcohol-coordinated porphyrin complex formation from TPPFeCl. The value of n is also four in this case. The coordination number 4 may be accounted for by hydrogen bonding between the iron-bound methanols and nearest neighbors contained in the excess of alcohol present in solution. This unusually high coordination number has also been obtained for TPPFe(imidazole)₂⁺Cl⁻ in benzene solution.¹⁰ The hydrogen bonding of the iron-bound aquo ligands

Table II. Equilibrium Constants for the Addition of Alcohols to the Ferric Complexes of Some Synthetic Porphyrins in CH₂Cl₂ at 21 °C

porphyrins	axial ligand	n^a	$\log \beta_n^b$	μ_{eff}^c
OEPFeCl	CH ₃ OH	3.9 ± 0.1	-2.3 ± 0.1	5.9 ± 0.3
OEPFeClO ₄	CH ₃ OH	2.3 ± 0.2	-2.3 ± 0.2	
TPPFeCl	CH ₃ OH	4.1 ± 0.2	-3.2 ± 0.1	5.9 ± 0.3
	C ₂ H ₅ OH	3.8 ± 0.2	-3.8 ± 0.1	5.9 ± 0.3

^a n as defined in eq 7. ^b β_n as defined in eq 7 was calculated from absorbance data taken at 391 and 540 nm for OEP, and 395 and 413 nm for TPP. ^c In μ_B at 24 °C.

with the tetrahydrofuran solvates, for TPPFe(H₂O)₂Cl⁻ 18 (as visualized from crystallographic study), also helps to substantiate the alcohol coordination number of 4. When OEPFeClO₄ is used in place of OEPFeCl, the resulting coordination number for alcohol is 2. This is presumably because the perchlorate anion may associate with the coordinated alcohols more readily than does the chloride anion and thus breaks the hydrogen bonding between the iron-bound and bulk alcohol molecules. It is worth noting that a fairly large excess of alcohol was required to form complex 2 from OEPFeCl and that, as Table II shows, the formation constant β_4 for TPPFe(CH₃OH)₄⁺Cl⁻ is substantially larger than that for TPPFe(C₂H₅OH)₄⁺Cl⁻. In other words, when alcohol substitutes the chloride of TPPFeCl to form the TPPFe(alcohol)₄⁺Cl⁻ complex, the concentration of alcohol required should be in the order methanol < ethanol ≈ propanol. This trend appears to be opposite to the order for the bulk dielectric constants (ϵ) of these alcohols,²⁷ $\epsilon(\text{CH}_3\text{OH}) = 33$, $\epsilon(\text{C}_2\text{H}_5\text{OH}) = 24$, and $\epsilon(\text{C}_3\text{H}_7\text{OH}) = 20$. This correspondence may allow us to expect that solvent polarity (ϵ) may facilitate the formation of the alcohol complex of ferric porphyrin (eq 7). Consequently, the step of Fe-Cl bond fission which is supposed to depend on the bulk solvent property (ϵ) is likely to be significant in the ligand substitution reaction. This is substantiated by the finding that complex 2 also forms from OEPFeClO₄ with a weak Fe-ClO₄ bond, in the presence of a small amount of methanol. Inspection of Table I shows that the α -CH₂ proton shift of complex 2 exhibits a slight downfield bias with respect to OEPFeCl and that it is almost insensitive to the variation of alcohol. Such features of the shifts are most probably due to the weak binding of alcohol to the iron atom.

The solution magnetic susceptibility of complex 2 corresponded to 5.9 μ_B for both OEPFe(CH₃OH)₄ and TPPFe(CH₃OH)₄ at 24 °C. These magnetic moments are independent of temperature between -40 and 24 °C. This value is characteristic of high-spin ferric TPPFeCl. On the basis of the proton hyperfine shifts and solution magnetic susceptibility data, it appears that complex 2 in CD₂Cl₂/CD₃OD is in the high-spin ferric state.

Table III. Observed Shifts^a for Ferric Octaethylporphyrin Complexes, [OEPFe(amine)(ROH)]⁺Cl⁻ ^b

alcohol	amine	pK _a ^c	α -CH ₂	β -CH ₃	meso-H	
CH ₃ OH ^d	piperidine	11.1	-33.8	-32.0 (-32.9) ^j	-5.2	35.0
CH ₃ OH ^e	piperidine	11.1	-34.1	-32.9 (-33.5) ^j	-5.2	34.7
CH ₃ OH ^d	pyrrolidine	11.1	-33.6	-31.1 (-32.4) ^j	-5.3	34.6
CH ₃ OH ^d	triethylamine	10.7	-34.5	-31.7 (-33.1) ^j	-5.3	
CH ₃ OH ^f	aziridine	8.0	-33.8			
C ₂ H ₅ OH ^g	piperidine	11.1	-33.6	-31.6 (-32.6) ^j	-5.2	36.0
C ₃ H ₇ OH ^h	piperidine	11.1	-33.1	-31.7 (-32.4) ⁱ	-5.0	35.5
CH ₃ OH ⁱ	4-Me ₂ Py	9.7	-34.1			33.0
CH ₃ OH ⁱ	1,2-Me ₂ Im	7.9	-34.7		-6.1	

^a Shifts in ppm (± 0.1) in CD₂Cl₂ at 21 °C, referenced against Me₄Si. ^b [OEPFeCl]₀ = 10.6 mM in each case. ^c In ref 34. ^d 1 μ L of CD₃OD (0.082 M). ^e 10 μ L of CD₃OD (0.82 M). ^f 6 μ L of CD₃OD (0.50 M) and 6.7 mM of aziridine. ^g 10 μ L of C₂D₅OD (0.58 M). ^h 10 μ L of C₃H₇OH (0.45 M). ⁱ 40-60 μ L of CD₃OD (2.3-3.5 M). ^j Mean values of two peaks.

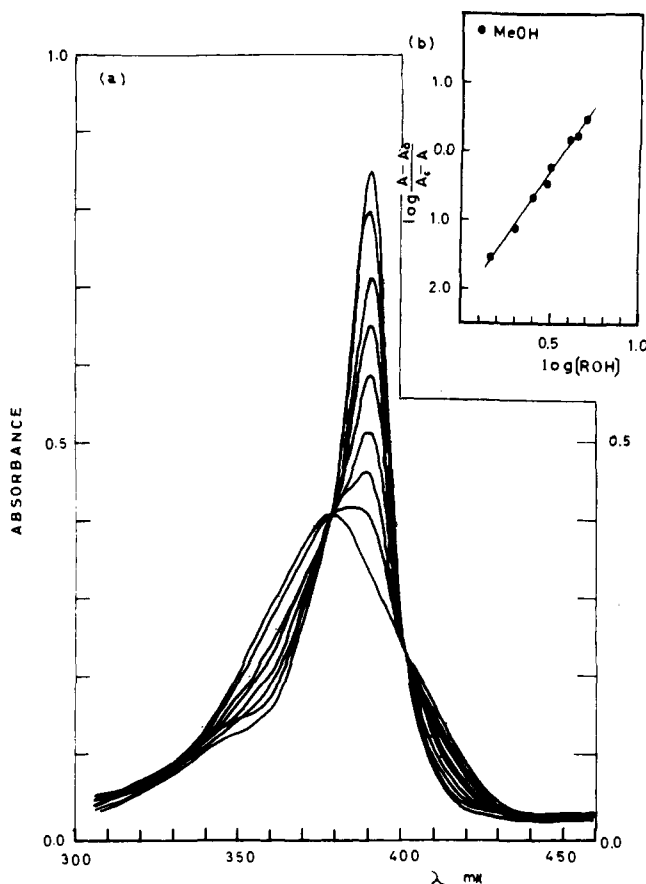


Figure 2. (a) Visible spectral changes for an 8.2×10^{-5} M solution of OEPFeCl in solvents consisting of CH₂Cl₂ and CH₃OH. (b) Method of analysis of absorbance data for the reaction of methanol with OEPFeCl in CH₂Cl₂.

(b) Formation of OEPFe(amine)(ROH)⁺Cl⁻ in Solution. The monoamine- and alcohol-coordinated porphyrin complexes were generated by adding an amine to a CD₂Cl₂ solution of OEPFeCl in the presence of a small amount of methanol. The ligand coordination reaction in this case follows eq 5. An increase in the concentration of amine displaces the equilibrium to the right. In Figure 3a the well-characterized proton spectrum of OEPFeCl in CD₂Cl₂ solution containing a small amount of methanol is illustrated. Addition of piperidine exhibits a remarkable effect on the spectrum: a new set of four peaks at -33.8, -32.0, -5.2, and 35.0 ppm with signal intensities of 2, 2, 6, and 1, respectively, was assigned to the α -H₂ doublet, β -CH₃, and meso-H of a newly generated single species. The four new peaks were not observed in the absence of alcohol; thus this new species (complex 4, Scheme I) may

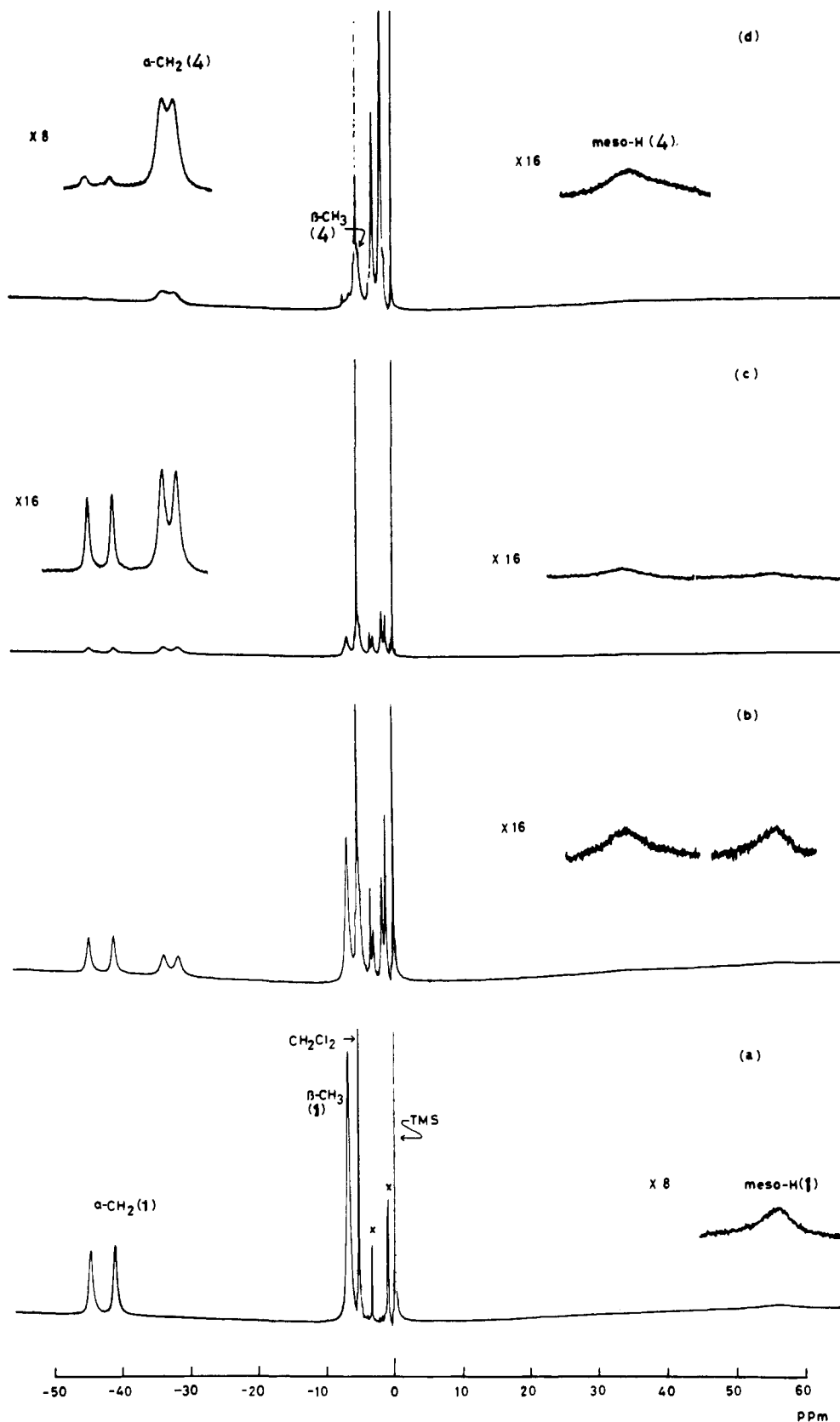


Figure 3. ^1H NMR spectra at 22 °C of a CD_2Cl_2 solution of 12 mM in total porphyrin, i.e., $[\text{OEPFeCl}]_0 = 12$ and 72 mM in total CD_3OD . The solution was titrated with piperidine: (a) 0; (b) 1.4; (c) 8.0; (d) 43; (e) 110 mM. The numbers 1 and 4 denote the species OEPFeCl and $\text{OEPFe}(\text{Pip})(\text{CH}_3\text{OH})^+\text{Cl}^-$, respectively.

be assigned to the porphyrin complex having methanol and piperidine as axial ligands. Doubling of the $\alpha\text{-CH}_2$ peak is, therefore, due to the diastereotopism²⁸ of this new complex in which different axial ligands remove the mirror plane sym-

metry to maintain the nonequivalence of the $\alpha\text{-CH}_2$ protons as was the case for $\text{OEPFe}(\text{imidazole})(\text{piperidine})$.²⁹ We have examined the formation of this mixed-ligand OEP complex with a variety of alcohols and amines. The observed proton

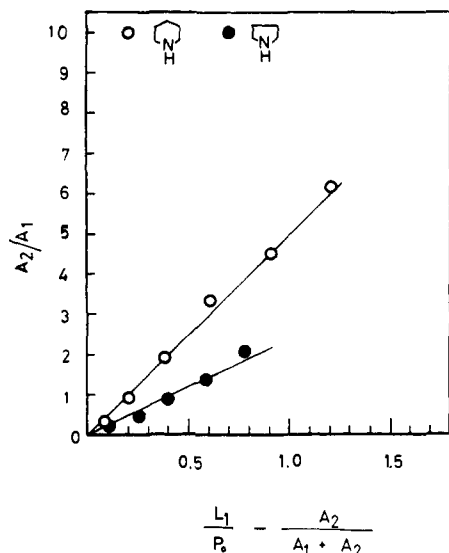


Figure 4. Method of analysis of peak intensities for ^1H NMR spectra of $\text{OEPFe}(\text{amine})(\text{CH}_3\text{OH})^+\text{Cl}^-$ (see footnote 31).

Table IV. Equilibrium Constants and Solution Susceptibility Data for $[\text{OEPFeL}_1\text{L}_2]^+\text{Cl}^-$ ^a

L_1^b	L_2	β_2^c	μ_{eff}^d
CH_3OH	piperidine	$(7.6 \pm 0.2) \times 10^2$	5.8 ± 0.2
CH_3OH	pyrrolidine	$(4.1 \pm 0.2) \times 10^2$	

^a $[\text{OEPFeCl}] = 8.2 \text{ mM}$ in CD_2Cl_2 solution. ^b $[\text{CD}_3\text{OD}] = 0.82 \text{ M}$. ^c β_2 as defined in eq 5, in units of M^{-2} . ^d In μ_B at $22 \pm 1^\circ\text{C}$.

shifts for these complexes are summarized in Table III.

Since the new peaks grow in intensity at their fixed positions with increasing concentration of amine, the ligand exchange rate is slow on the NMR time scale. Hence, the equilibrium constants were readily computed from the relative intensities of the α - CH_2 doublet peaks of OEPFeCl and $\text{OEPFe}(\text{CH}_3\text{OH})(\text{piperidine})^+$. The equilibrium³⁰ stoichiometry in eq 5 affords β_2 when amine ($[\text{L}_1]$) is added to the OEPFeCl solution containing a small amount of methanol (0.8 M). The method of analysis is given in footnote 31 and is shown in Figure 4. The calculated β_2 values (listed in Table IV) are about 10^2 M^{-2} , which is comparable to that obtained by Satterlee et al.⁹ for the formation of $\text{OEPFe}(\text{1-MeIm})_2^+\text{Cl}^-$ from OEPFeCl in CHCl_3 .

(c) **Equilibria in the Formation of Six-Coordinated High-Spin Ferric Porphyrin Complexes in the Presence of Amine and Alcohol.** Based on the observations in Figures 1 and 3 and eq 1–7, Scheme 1 is now proposed for the process of formation of $\text{OEPFeL}_1\text{L}_2^+\text{Cl}^-$ in CD_2Cl_2 solution. In the previous section, we have discussed the processes labeled A and B in Scheme 1 by which complexes 2 and 4 are formed, respectively. Complex 4 is also generated from complex 2 by process D. Figure 5 (1) shows the well-resolved ^1H NMR spectrum of complex 2. Successive addition of piperidine causes upfield shifts for the α - CH_2 and β - CH_3 proton peaks and a downfield shift for the meso-H resonance, respectively. The formation of complex 4 is exemplified in Figure 5 (5). As Figure 5 (5) shows, the singlet signal is obtained for the α - CH_2 group of complex 4 in the presence of a large excess of alcohol, indicating that rapid chemical exchange occurs. When complex 4 is formed by process B, further addition of alcohol displaces the equilibrium between complexes 2 and 4 in Scheme 1 to the left, so that complex 2 is also formed from complex 4.

Although the six-coordinate piperidine complex 3 can be formed by process C, its ferric iron is reduced automatically

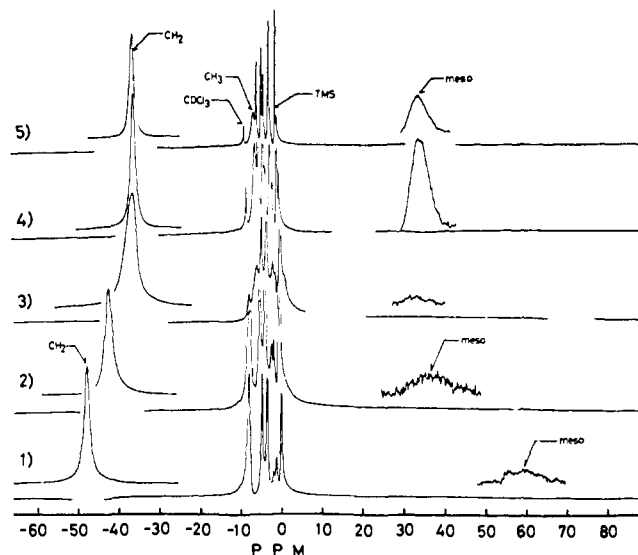
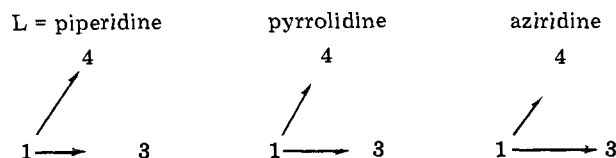


Figure 5. ^1H NMR spectra at 21°C of $\text{CDCl}_3/\text{CD}_3\text{OD}$ (4:3, v/v) solution of 27.5 mM in total OEPFeCl . The solution was titrated with piperidine: (1) 0; (2) 10; (3) 30; (4) 71; (5) 170 mM.

Scheme II



in the presence of a large amount of amine.³² However, by process E in Scheme 1 the bisamine complex 3 in the ferric low-spin state is formed without reduction of the iron atom. Thus, complex 3 is formed by adding relatively large amounts of piperidine at low temperatures.³³

A negligible amount of complex 4 was formed with some amines. Figure 6 shows the formation of complexes 3 and 4 in the presence of methanol and aziridine at 21°C . Addition of aziridine to a solution of 11 mM OEPFeCl and 80 mM methanol yielded the bisamine complex 3 rather than the mixed-ligand complex 4 (Figure 6b). A relatively large amount of methanol was required to form $\text{OEPFe}(\text{aziridine})(\text{CH}_3\text{OH})^+\text{Cl}^-$ (Figures 6c and 6d). Scheme II represents the formation of complexes 3 and 4, which depends upon the choice of amine in the presence of an equal amount of alcohol. In the case of piperidine, complex 4 is selectively generated, while complex 3 is predominantly formed by the use of aziridine. As Table IV shows, the value of $\beta_2(\text{Pip})$ for the formation of $\text{OEPFe}(\text{CH}_3\text{OH})(\text{Pip})^+\text{Cl}^-$ by process B is twice as large as $\beta_2(\text{Pyrr})$. This trend appears to correspond to the relative basicities of the amines in the order $\beta_2(\text{Pip}) \approx \beta_2(\text{Pyrr}) \gg \beta_2(\text{Az})$. Consequently, the stability of complex 4 may be determined by the basicity of the amine. The correlation between basicity of the axial ligand and the complex formation constant, β_2 , is also found for low-spin ferric porphyrin complexes of N-substituted imidazoles.^{9,10} It is thus tempting to conclude that stabilization of the positive charge on $\text{Fe}(\text{III})$ by the axial ligands appears to be an important structural factor for the production of the mixed ligand complex 4 in solution.

(d) **Properties of Monoamine Ferric OEP Complexes in Relation to the Model of Aquometmyoglobin.** We are now concerned with the properties of the mixed-ligand high-spin ferric complex 4 in relevance to the physical properties of the ferric porphyrin moiety in ferric hemoproteins. The effective magnetic moment of $\text{OEPFe}(\text{Pip})(\text{CH}_3\text{OH})^+\text{Cl}^-$ in CDCl_3 solution is found to be $5.8 \mu_B$ at 21°C (Table IV), which is in

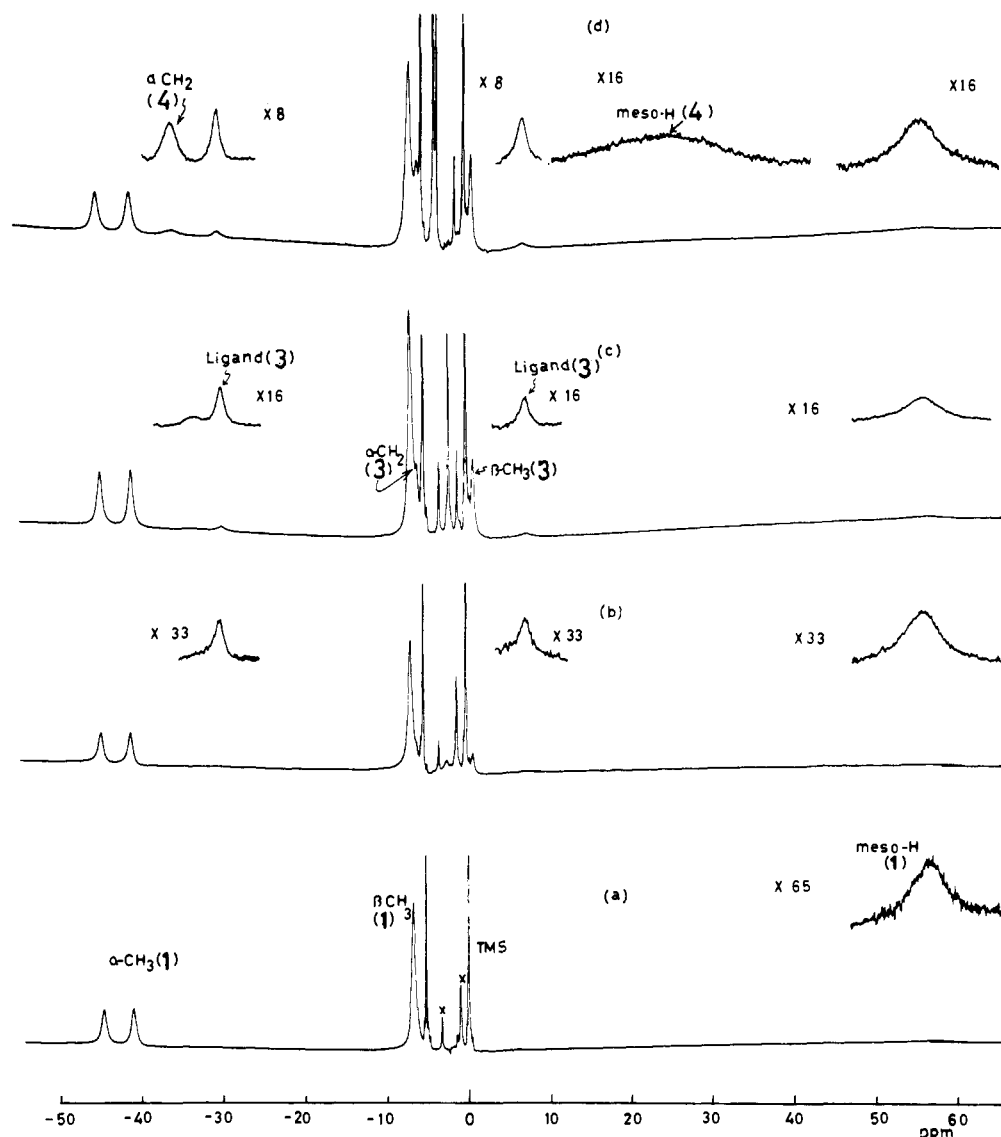


Figure 6. ^1H NMR spectra at 21 °C of a CD_2Cl_2 solution of 10.8 mM in total OEPFeCl : (a) $[\text{CD}_3\text{OD}]_0 = 73$ mM; (b) $[\text{CD}_3\text{OD}]_0 = 73$ mM and $[\text{aziridine}]_0 = 6.7$ mM; (c) $[\text{CD}_3\text{OD}]_0 = 430$ mM and $[\text{aziridine}]_0 = 6.7$ mM; (d) $[\text{CD}_3\text{OD}]_0 = 3.1$ M and $[\text{aziridine}]_0 = 6.7$ mM.

good agreement with the spin-only moment of $5.9 \mu_B$ observed for five-coordinate high-spin ($S = 5/2$) ferric porphyrins. To examine whether or not complex **4** resides in a single spin state, we have measured the temperature dependence of the isotropic shift ranging from 40 to -50 °C (Figure 7).

Figure 7 shows an apparently linear relation for all of the resonances of complex **4**, which is characteristic of a single spin state. Hence, $\text{OEPFe}(\text{CH}_3\text{OH})(\text{Pip})^+\text{Cl}^-$ can be assigned as a pure high-spin ($S = 5/2$) ferric complex. This contrasts with the low-spin six coordinate complex, $^{16}\text{FePPIXDEBL}_1\text{L}_2$ ($\text{L}_1 = \text{phenoxide}$ and $\text{L}_2 = \text{pyridine}$ or imidazole). The combination of weak and moderate field ligands (CH_3OH and piperidine) employed here has allowed us to reproduce a six-coordinate high-spin ferric porphyrin complex, which is a suitable model for aquomet-Hb and -Mb.

It is worth noting in Tables I and III that all of the observed $\alpha\text{-CH}_2$, $\beta\text{-CH}_3$, and meso-H shifts of $\text{OEPFe}(\text{CH}_3\text{OH})(\text{Pip})^+\text{Cl}^-$ are considerably smaller than those of OEPFeCl and $\text{OEPFe}(\text{ROH})_2^+\text{Cl}^-$. This is qualitatively interpreted³⁵ in terms of a competitive balance between iron-porphyrin binding and iron-axial ligand binding in high-spin complexes. When an axial ligand has a high affinity for the ferric iron, the iron-porphyrin interaction is weakened and consequently smaller shifts of the porphyrin resonances are observed. The

present results, concerning the relative magnitudes of the hyperfine shifts for the high-spin $\text{OEPFe}(\text{CH}_3\text{OH})(\text{Pip})^+\text{Cl}^-$ and $\text{OEPFe}(\text{CH}_3\text{OH})_2^+\text{Cl}^-$ complexes, are attributable to differences in the strengths of the iron-porphyrin and iron-axial ligand bonds in these complexes.

Furthermore, as shown in Table III, the porphyrin resonances for $\text{OEPFe}(\text{ROH})(\text{amine})^+\text{Cl}^-$ are not affected by the weak perturbation produced by the varying basicities of the amines ($\text{p}K_a = 10\text{--}11$) and alcohols at the axial positions. The combination of axial ligands (alcohol/amine) appears to be intrinsically responsible for the differences in the observed isotropic shifts.

With the aim of gaining insight into the nature of iron-nitrogenous base bonding, we have attempted here to obtain the mixed ligand complexes with imidazole, or its derivatives, at the fifth position that are more relevant structural models for aquomet-Mb. The corresponding pyridine complexes were also examined. Among the imidazole derivatives only hindered imidazoles (2-methylimidazole, 1,2-dimethylimidazole, and benzimidazole) yielded mixed ligand complexes whose ^1H NMR spectra exhibit a chemical exchange effect due to labile ligation of these ligands to the iron (see Figure 8). The other imidazole derivatives examined led to low-spin bis adducts. In the case of pyridine derivatives, only a *N,N*-dimethylamino-

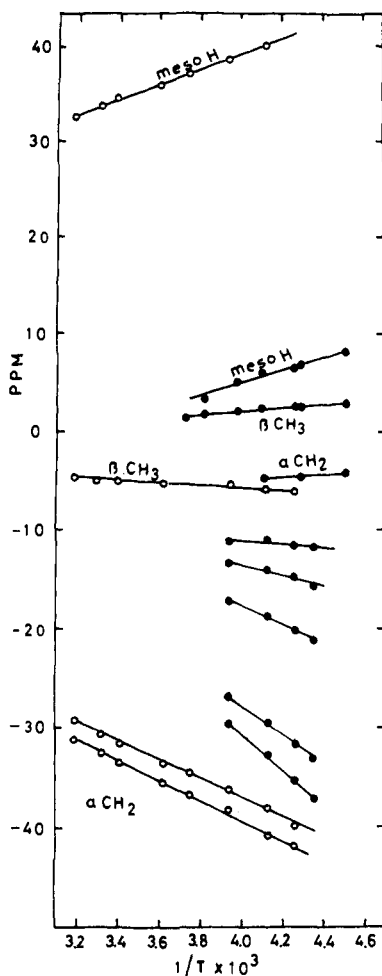


Figure 7. Temperature dependence of the observed shift of the protons of $\text{OEPFe(Pip)(CH}_3\text{OH)}^+\text{Cl}^-$ (○) and $\text{OEPFe(Pip)}_2^+\text{Cl}^-$ (●).

pyridine, which has a high basicity compared with the other pyridine derivatives, selectively yielded the desired mixed-ligand high-spin complexes. The other pyridine derivatives produced low-spin bis adducts. The complexes associated with the hindered imidazoles showed porphyrin ^1H resonances averaged by chemical exchange effects. A similar observation was made for a high-spin complex $\text{OEPFe(Az)(CH}_3\text{OH)}^+\text{Cl}^-$ (Figure 7). The observed $\alpha\text{-CH}_2$ shift was -34 ppm for 2-Melm, close to the shift for aziridine in Table III. Consequently, when imidazoles are used as axial bases at the fifth position of a high-spin ferric porphyrin complex, the sterically hindered interaction between the substituted group on the ligand molecule and the porphyrin ring appears to be important enough to allow the formation of an alcohol-imidazole adduct of high-spin ferric porphyrin complexes. This implies that a delicate balance of axial ligation modes is needed to form mixed-ligand high-spin ferric porphyrin complexes.

The NMR study reported herein demonstrates a new structural type for high-spin ferric porphyrins in solution. Although the high-spin ferric mixed-ligand porphyrin complexes studied here are largely concerned with nonimidazole nitrogenous bases, the alcohol-amine containing porphyrin complex is expected to serve as a structural model for aquometmyoglobin and aquomethemoglobin. We are currently studying the hyperfine-shifted ^1H NMR spectra of high-spin ferric hemoproteins in order to delineate the heme microenvironmental structures in relation to their biological functions.³⁶ In connection with this, our present study on a new type of high-spin ferric complex is being extended to a natural porphyrin, namely protoporphyrin dimethyl ester.

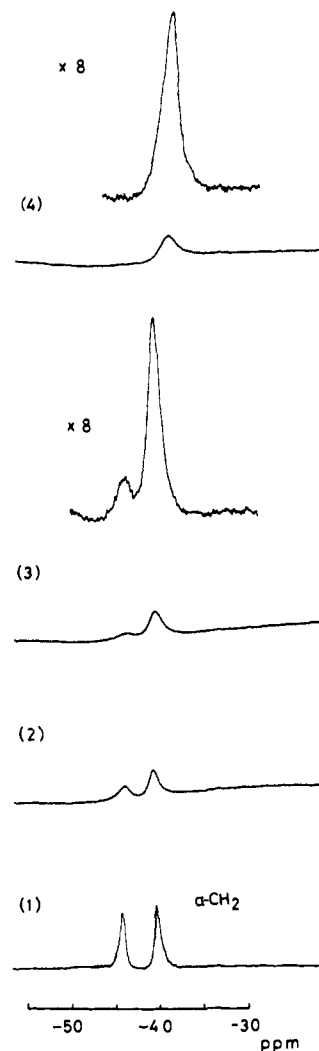


Figure 8. ^1H NMR spectra of the downfield region at 22°C of a CDCl_3 solution of 8.7 mM in total porphyrin, i.e., $[\text{OEPFeCl}]_0 = 8.7$ mM and $[\text{CD}_3\text{OD}]_0 = 1.6$ M. The observed shift is referenced against internal $(\text{Me})_4\text{Si}$. The solution was titrated with 2-methylimidazole: (1) 0; (2) 8; (3) 12; (4) 20 mM. The intensity of the $\alpha\text{-CH}_2$ signal for OEPFeCl decreases and a new signal at -41 ppm increases simultaneously. The new signal is assigned to the $\alpha\text{-CH}_2$ group of a mixed-ligand complex. This signal shifts upfield with an increase of $[\text{2-Melm}]$. The concentration dependence of this shift is different from the case that occurs in the absence of methanol.

Acknowledgment. This work was supported by grants from the Ministry of Education, Japan (No. 354139), and from the Toray Science Foundation. The authors are grateful to Professor T. Yonezawa for continuous encouragement.

References and Notes

- (1) Taken in part from: Kitagawa, S. Ph.D. Thesis, Kyoto University, Kyoto, submitted for publication. Department of Chemistry, Faculty of Science and Technology, Kinki University, Kowakae, Higashi-Osaka, Japan.
- (2) Department of Biochemistry and Biophysics, University of Pennsylvania School of Medicine, Philadelphia, Pa.
- (3) Antonini, E.; Brunori, M. "Hemoglobin and Myoglobin in Their Reactions with Ligands"; North-Holland: Amsterdam, 1971.
- (4) Eichhorn, G., Ed. "Inorganic Biochemistry"; Elsevier: Amsterdam, 1973.
- (5) Lemberg, R; Barrett, J. "Cytochromes"; Academic Press: New York, 1973.
- (6) Smith, K. M., Ed., "Porphyrins and Metalloporphyrins"; Elsevier: Amsterdam, 1975.
- (7) Hill, H. A. O.; Morallee, K. G. *J. Am. Chem. Soc.* **1972**, *94*, 731.
- (8) Satterlee, J. D.; LaMar, G. N. *J. Am. Chem. Soc.* **1976**, *98*, 2804.
- (9) Satterlee, J. D.; LaMar, G. N.; Frye, J. S. *J. Am. Chem. Soc.* **1976**, *98*, 7275.
- (10) Walker, F. A.; Lo, M. W.; Ree, M. T. *J. Am. Chem. Soc.* **1976**, *98*, 5552.
- (11) LaMar, G. N.; Frye, J. S.; Satterlee, J. D. *Biochim. Biophys. Acta* **1976**, *428*, 78.

- (12) LaMar, G. N.; Bold, T. J.; Satterlee, J. D. *Biochim. Biophys. Acta* **1977**, *498*, 189.
- (13) Satterlee, J. D.; LaMar, G. N.; Bold, T. J. *J. Am. Chem. Soc.* **1977**, *99*, 1088.
- (14) Buchler, J. W. In ref 4, Chapter 5.
- (15) LaMar, G. N.; Eaton, G. R.; Holm, R. H.; Walker, F. A. *J. Am. Chem. Soc.* **1973**, *95*, 63.
- (16) Ainscough, E. W.; Addison, A. W.; Dolphin, D.; James, B. R. *J. Am. Chem. Soc.* **1978**, *100*, 7585.
- (17) Hoard, J. L. In ref 4, Chapter 8.
- (18) Kastner, M. E.; Scheidt, W. R.; Mashiko, T.; Reed, C. A. *J. Am. Chem. Soc.* **1978**, *100*, 666.
- (19) Abbreviations used in this paper are: tPP, dianion of tetraphenylporphyrin; OEP, dianion of octaethylporphyrin; Pip, piperidine; Pyr, pyrrolidine; Az, aziridine.
- (20) Mashiko, T.; Kastner, M. E.; Spatallian, K.; Scheidt, W. R.; Reed, C. A. *J. Am. Chem. Soc.* **1978**, *100*, 6354.
- (21) Zobrist, M.; LaMar, G. N. *J. Am. Chem. Soc.* **1978**, *100*, 1944.
- (22) Whitlock, H. W.; Hanauer, R. *J. Org. Chem.* **1968**, *33*, 2169.
- (23) Whitlock, H. W.; Hanauer, R.; Oester, M. Y.; Bauer, B. K. *J. Am. Chem. Soc.* **1969**, *91*, 7486.
- (24) Falk, J. E. "Porphyrins and Metalloporphyrins"; Elsevier: New York, 1964.
- (25) Evans, D. F. *J. Chem. Soc.* **1959**, 2003.
- (26) In the presence of a large amount of alcohol, the following relation⁸ holds for the formation of $\text{PFe}(\text{ROH})_n^+\text{Cl}^-$: $\log R = n \log [\text{ROH}] + \log \beta_n$, where $R = [A - A_0/A_c - A]$.
- (27) Riddick, J. A.; Bunger, W. B. "Techniques of Chemistry"; Wiley-Interscience: New York, 1970; Vol. II.
- (28) Walker, F. A.; LaMar, G. N. *Ann. N.Y. Acad. Sci.* **1973**, *206*, 328.
- (29) Morishima, I.; Masuda, H.; Kitagawa, S., manuscript in preparation.
- (30) In the case of $L_1 = \text{piperidine}$ and $L_2 = \text{methanol}$, the dominant species is a mixed-ligand complex in the presence of a small amount of alcohol.
- (31) Details of the calculation are as follows: A_1 and A_2 are signal areas of the $\alpha\text{-CH}_2$ resonances of OEPFeCl and $\text{OEPFe}(\text{Pip})(\text{CH}_3\text{OH})^+\text{Cl}^-$, respectively, where $A_2/A_1 (= Y)$ must be equal to $[\text{OEPFe}(\text{Pip})(\text{CH}_3\text{OH})^+\text{Cl}^-]/[\text{OEPFeCl}]$ under the conditions of slow exchange between these complexes. In the presence of an excess of methanol, $[\text{CH}_3\text{OH}] \gg [\text{P}]_0$, the following relation is obtained with the use of notations ($L_1 = \text{piperidine}$; $[\text{P}]_0 = [\text{OEPFeCl}]_0$; $Y = \beta_2[\text{CH}_3\text{OH}][\text{P}]_0([\text{L}_1]_0/[\text{P}]_0 - A_2/(A_1 + A_2))$, where the R value is plotted against $([\text{L}_1]_0/[\text{P}]_0 - A_2/A_1 + A_2)$. If the above approximation is correct, a linear relation will be obtained (see Figure 4) and its extrapolation to $([\text{L}_1]_0/[\text{P}]_0 - A_2/A_1 + A_2) \rightarrow 0$ shows a zero intercept, and the slope is $\beta_2[\text{CH}_3\text{OH}][\text{P}]_0$.
- (32) Gaudio, J. D.; LaMar, G. N. *J. Am. Chem. Soc.* **1976**, *100*, 1112.
- (33) Morishima, I.; Kitagawa, S.; Hisamatsu, M.; Masuda, H., manuscript in preparation.
- (34) Perrin, D. D. "Dissociation Constants in Organic Bases in Aqueous Solution"; Butterworths: London, 1965.
- (35) In low-spin bis(4-substituted pyridine) complexes, the isotropic shift for the porphyrin pyrrole proton does not necessarily reflect the bonding strength of iron-axial ligand binding: bispyridinates of natural porphyrins⁷ exhibited hyperfine shifts of the peripheral proton groups that increase significantly with lower basicity of the pyridine derivatives, while those of the pyrrole proton of TPP¹² show the opposite trend.
- (37) Morishima, I.; Ogawa, S.; Inubushi, T.; Iizuka, T. *Adv. Biophys.* **1978**, *11*, 217. Morishima, I.; Neya, S.; Inubushi, T.; Yonezawa, T.; Iizuka, T. *Biochim. Biophys. Acta* **1978**, *534*, 307. Morishima, I.; Ogawa, S.; Inubushi, T.; Yonezawa, T.; Iizuka, T. *Biochemistry* **1977**, *16*, 5109. Morishima, I.; Ogawa, S. *J. Biol. Chem.* **1979**, *254*, 2814. Neya, S.; Morishima, I. *J. Biol. Chem.* **1979**, *254*, 9107. Neya, S.; Morishima, I. *Biochemistry*, in press.

Bacteriochlorophylls *c* from *Chloropseudomonas ethylicum*. Composition and NMR Studies of the Pheophorbides and Derivatives

Kevin M. Smith,*^{1a} Michael J. Bushell,^{1a} John Rimmer,^{1b} and John F. Unsworth^{1b}

Contribution from the Department of Chemistry, University of California at Davis, Davis, California 95616, and The Robert Robinson Laboratories, University of Liverpool, Liverpool, England. Received September 17, 1979

Abstract: The carbon-13 and proton NMR spectra of the methyl pheophorbides **6**, methyl 2-vinylpheophorbides **2**, methyl mesopheophorbides **7**, and other degradation products from the green sulfur bacterium *Chloropseudomonas ethylicum* are described and assigned. In order to clarify certain spectra, model chlorins substituted with *n*-propyl, isobutyl, propenyl, and isobutenyl side chains are synthesized from the chlorophyll *b* degradation product, rhodin *g*₇ trimethyl ester (**17**). Successful separations of the homologous mixture of pheophorbides, using reverse-phase high-performance liquid chromatography, are detailed; only four major bands (rather than the six obtained from *Chlorobium thiosulfatophilum* cultures) were observed, and only a minute amount of 4-ethyl-5-methylpheophorbide (band **6**) was apparent in the *C. ethylicum* culture presently being studied.

The bacteriochlorophylls *c* (*Chlorobium* chlorophylls 660) from various green sulfur bacteria (Chlorobiaceae) have been extensively investigated. The structures shown in **1** have been assigned to the homologues in the mixture of bands, but those assigned to bands 1 and 3 (**1a** and **1c**, respectively) must be regarded as tenuous, since there exists no positive evidence for δ meso groups other than methyl.² Recently, Brockmann has described the isolation of a series of 3-formylchlorophylls (bacteriochlorophylls *e*)³ and chlorophylls with esterifying alcohols other than farnesol,⁴ and, again, in no case was a δ meso ethyl substituent observed.

In earlier papers^{2b,5} we described initial studies on the biosynthesis of the *Chlorobium* chlorophylls from *Chloropseudomonas ethylicum*,⁶ and several novel chemical transformations of these chlorophylls were described. In particular, a unique vinyl cyclization (**2** \rightarrow **3**) and a photooxidative ring opening (**4** \rightarrow **5**) were characterized. The 2 + 2 addition of oxygen to a macrocyclic double bond, which we proposed,^{2b} has recently been confirmed by Risch,⁷ and by ourselves, and

we have carried out experiments with chlorin models that indicate that the specificity of the oxidative cleavage, which gives only one photobilin isomer, **5**, is controlled by the presence of the cyclopentanone ring.⁸ In the present paper we describe the mass and NMR spectra of the pheophorbides and derivatives from *Chloropseudomonas ethylicum*,⁶ and describe our ultimately successful attempts at separation of the homologous mixture. Our previous NMR assignments^{2b} of the *n*-propyl and isobutyl groups had depended upon comparisons with *n*-propyl- and isobutylbenzenes. Owing to the fact that chlorophylls and porphyrins (unlike simple benzenoid compounds) undergo extensive aggregation phenomena⁹ which affect observed chemical shifts, we also describe the partial syntheses of *n*-propyl and isobutyl derivatives (from pheophytin *b*) which enable a better estimation of the NMR parameters of these substituents in the homologous mixture.

Field Desorption Mass Spectra

Using *Chlorobium thiosulfatophilum*, Holt and co-work-